Chapter 4

The Fundamental Gap in RDMFT

The theoretical description of atoms, molecules, and solids relies on the calculation of single-particle orbitals, like Hartree-Fock or Kohn-Sham orbitals, and their respective energies. Experimentally extensive information is obtained from photo-emission and -absorption spectra. In photo-absorption experiments one measures the difference between the ground-state and an excited state of an N-particle system by measuring the energy of a photon which is absorbed by the system. The difference between the ground-state energy and the first excited state

$$\tilde{\Delta} = E^{gs}_{\text{total}}(N) - E^{exc}_{\text{total}}(N) \tag{4.1}$$

is called the optical or neutral gap of the system. As a second possibility, one can ionize the system in a photo-emission experiment. The absorbed photon in this case has enough energy to allow an electron to leave the system. From the known energy of the photon and the measured energy of the escaping electron one can obtain the ionization potential

$$I = E_{\text{total}}(N-1) - E_{\text{total}}(N). \tag{4.2}$$

Additionally, one can measure the electron affinity

$$A = E_{\text{total}}(N) - E_{\text{total}}(N+1) \tag{4.3}$$

from an inverse photo-emission experiment, where an electron is absorbed by the system and the energy of the resulting photon is measured. The fundamental gap of the system is defined as

$$\Delta = I - A. \tag{4.4}$$

In the chemistry literature (e.g. Ref. [45]), $\Delta/2$ is usually termed the absolute hardness of a chemical species. Here, we use the term fundamental gap for both finite and extended systems since the physical concept defined by Eq. (4.4) is the same in both cases.

The fundamental gap Δ differs from the optical gap $\tilde{\Delta}$ because of the attractive interaction between the electron and the corresponding hole which is part of the

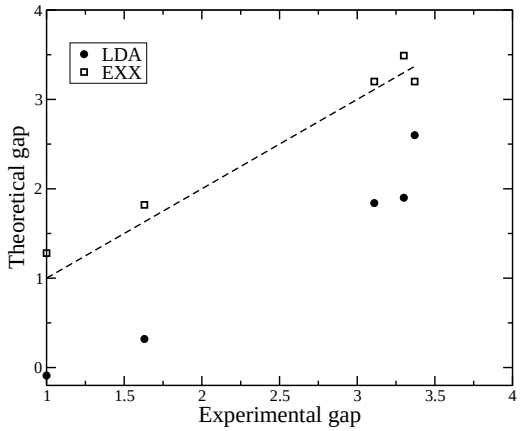

Figure 4.1: The KS gap at the Γ point for Ge, GaAs, AlAs, GaN, and Si (left to right) calculated from LDA and exact exchange. The dashed line is a guide to the eye for the experimental value. Numbers are taken from Refs. [15, 44]

optical gap. Therefore, the optical gap is smaller than the fundamental one by the binding energy of the resulting exciton in the photo-absorption experiment.

In DFT the fundamental gap is given by

$$\Delta = \Delta_{KS} + \lim_{\eta \to 0} \left(\left. \frac{\delta E_{xc}}{\delta n(\mathbf{r})} \right|_{N+\eta} - \left. \frac{\delta E_{xc}}{\delta n(\mathbf{r})} \right|_{N-\eta} \right). \tag{4.5}$$

However, as already mentioned in the introduction, employing the commonly used LDA leads to a gap which is 30-100% too small. The discrepancy is due to the derivative discontinuity of the exchange-correlation energy which is not described by LDA. The band gap is therefore solely given by the KS band gap. Fig. 4.1 shows the results for several semi-conducting systems. Although all LDA results are too small the largest error occurs in Germanium which is even predicted as a metal in LDA. Using the exact-exchange functional the KS band gap is in quite good agreement with experimental values, see Fig. 4.1. It was shown, however, that the agreement is due to a fortuitous cancellation of errors in these systems and does not hold in general [11]. In addition, the derivative discontinuity of the exact-exchange functional is different from zero. Adding it properly leads to a gap very close to the HF gap which is therefore too large.

In this chapter we are concerned with the fundamental gap of finite and periodic systems and how to calculate it within reduced-density-matrix-functional theory. In Section 4.1 we present the formalism for the calculation of the fundamental gap. Special attention needs to be paid to the N-representability problem to be covered in Section 4.2. We then focus on the numerical implementation and close the chapter with results for finite as well as periodic systems in Section 4.3.

4.1 The Fundamental Gap as the Discontinuity of the Chemical Potential

In order to derive the fundamental gap (4.4) within RDMFT we extend the definition of the total-energy functional $E_{\text{total}}[\Gamma^{(1)}]$ to systems with fractional particle number M. Such systems can be described as an ensemble consisting of an N- and an $(N+1)$-particle state for $N \leq M \leq N+1$. The expectation value O of an operator $\hat{O}$ is then given by the trace

$$O = tr(\hat{D}\hat{O}), \tag{4.6}$$

where $\hat{D}$ is the statistical matrix. In the case of an ensemble of an N- and an $(N+1)$-particle state it is given by

$$\hat{D} = \alpha_N \,|\,\Psi^N\rangle\langle\Psi^N\,|\, + \alpha_{N+1}\,|\,\Psi^{N+1}\rangle\langle\Psi^{N+1}\,|, \tag{4.7}$$

where Ψ^N and Ψ^{N+1} represent the N- and $(N+1)$-particle wave functions which contribute to the ensemble. The ensemble 1-RDM for fractional particle number is therefore given by

$$\begin{aligned}\Gamma^{(1)M}(\mathbf{x};\mathbf{x}') &= tr(\hat{D}\hat{\Gamma}^{(1)}) \\ &= \alpha_N N \int d\mathbf{x}_2 ... d\mathbf{x}_N \; \Psi^{N*}(\mathbf{x}', \mathbf{x}_2 ... \mathbf{x}_N)\Psi^N(\mathbf{x}, \mathbf{x}_2 ... \mathbf{x}_N) \\ &\quad + \alpha_{N+1}(N+1) \int d\mathbf{x}_2 ... d\mathbf{x}_{N+1} \; \Psi^{N+1*}(\mathbf{x}', \mathbf{x}_2 ... \mathbf{x}_{N+1})\Psi^{N+1}(\mathbf{x}, \mathbf{x}_2 ... \mathbf{x}_{N+1}) \; .\end{aligned} \tag{4.8}$$

Since the density, i.e. the diagonal of the 1-RDM, has to integrate to the particle number $M = N + \eta$ ($N \in \mathbb{N}$, $0 \leq \eta \leq 1$) the coefficients α_N and α_{N+1} have to take the values

$$\alpha_N = 1 - \eta \tag{4.9}$$

$$\alpha_{N+1} = \eta. \tag{4.10}$$

The resulting ensemble 1-RDM then reduces to

$$\Gamma^{(1)M}(\mathbf{x};\mathbf{x}') = (1-\eta)\,\Gamma^{(1)N}(\mathbf{x};\mathbf{x}') + \eta\,\Gamma^{(1)N+1}(\mathbf{x};\mathbf{x}'). \tag{4.11}$$

The ground-state energy of the ensemble is

$$E_{\text{total}}(M) = (1-\eta)E_{\text{total}}(N) + \eta E_{\text{total}}(N+1), \tag{4.12}$$

where $E_{\text{total}}(N)$ and $E_{\text{total}}(N+1)$ are the ground-state energies of the N- and $(N+1)$-particle system, respectively. Fig. 4.2 shows the total energy as a function of η, or alternatively as a function of the fractional particle number M. One can verify this picture by reformulating (4.12) as

$$E_{\text{total}}(M) = E(N) + \eta\,[E(N+1) - E(N)] \tag{4.13}$$

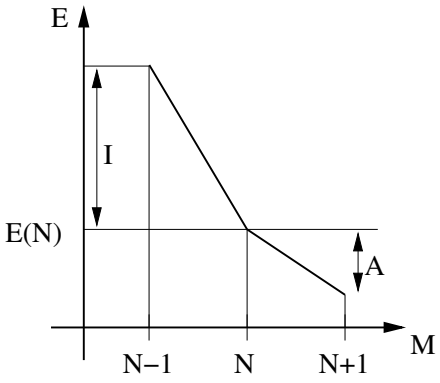

Figure 4.2: Total energy for a fractional total number of particles M. The energy shows a derivative discontinuity at integer particle number N. The ionization potential I and the electron affinity A are also given.

for $N < M < N + 1$. For $N - 1 < M < N$, one obtains in analogy

$$E_{\text{total}}(M) = E(N-1) + \eta \left[E(N) - E(N-1) \right]. \tag{4.14}$$

Since $A = E(N+1) - E(N)$ and $I = E(N) - E(N-1)$ are in general not the same, the derivative $\partial E_{\text{total}}(M)/\partial M$ has a discontinuity at integer particle number N. For Coulomb-systems Lieb's conjecture claims that the energy is a convex function of the particle number such that the electron affinity is smaller than the ionization potential [46]. From Eqs.(4.2-4.4), one can conclude that the derivative discontinuity of the energy is identical to the fundamental gap

$$\Delta = \left. \frac{\partial E_{\text{total}}(M)}{\partial M} \right|_{N+\eta} - \left. \frac{\partial E_{\text{total}}(M)}{\partial M} \right|_{N-\eta}. \tag{4.15}$$

The total energy of a system in RDMFT is calculated by minimizing the functional (2.58)

$$F[\Gamma^{(1)}] = E_{\text{total}}[\Gamma^{(1)}] - \mu \left(\int d\mathbf{x}\, \Gamma^{(1)}(\mathbf{x};\mathbf{x}) - N \right). \tag{4.16}$$

For fractional particle number M the question again arises when the one-body reduced density matrix $\Gamma^{(1)}$ is N-representable. Here, N-representability refers to Eq. (4.11), i.e. is it possible to write the density matrix as a weighted sum of two density matrices for integer particle numbers which are themselves N-representable? As we show in the next section this is ensured again by restricting the occupation numbers of the M-particle system to the interval $[0;1]$ and ensure $\sum_j n_j = M$. Here, we continue to discuss the fundamental gap using this constraint.

First, we prove that the Lagrangian multiplier μ in equation (4.16) is nothing else but the chemical potential, i.e.

$$\mu(M) = \frac{\partial E_{\text{total}}(M)}{\partial M}. \tag{4.17}$$

This is not at all obvious because, in contrast to DFT, $\delta F/\delta\Gamma^{(1)}$ does not need to vanish at the minimum energy due to the states pinned at the border. As discussed in Section 2.5, for these states the occupation number is pinned to either zero or one in order to satisfy the N-representability constraint. The minimum is hence a border minimum with non-vanishing derivative. To prove (4.17) nevertheless, we investigate the difference

$$E_{\text{total}}(M+\eta) - E_{\text{total}}(M) = E[\Gamma^{(1)M+\eta}] - E[\Gamma^{(1)M}], \tag{4.18}$$

where $\Gamma^{(1)M+\eta}(\mathbf{x};\mathbf{x}')$ and $\Gamma^{(1)M}(\mathbf{x};\mathbf{x}')$ denote the ground-state density matrices of the $M+\eta$ and M particle systems, respectively. A Taylor expansion of $E[\Gamma^{(1)M+\eta}]$ around $\Gamma^{(1)M}$ leads to

$$E_{\text{total}}(M+\eta)-E_{\text{total}}(M) = \iint d\mathbf{x}d\mathbf{x}' \frac{\delta E_{\text{total}}}{\delta\Gamma^{(1)}(\mathbf{x};\mathbf{x}')}\bigg|_{\Gamma^{(1)M}} \left(\Gamma^{(1)M+\eta}(\mathbf{x};\mathbf{x}') - \Gamma^{(1)M}(\mathbf{x};\mathbf{x}')\right), \tag{4.19}$$

where we only kept terms up to first order in the density matrices. The functional derivative of (4.16) yields

$$\frac{\delta F}{\delta\Gamma^{(1)}(\mathbf{x};\mathbf{x}')} = \frac{\delta E_{\text{total}}}{\delta\Gamma^{(1)}(\mathbf{x};\mathbf{x}')} - \mu\delta(\mathbf{x}-\mathbf{x}'). \tag{4.20}$$

Evaluating $\delta F/\delta\Gamma^{(1)}$ via the functional chain rule with respect to the occupation numbers n_j and the natural orbitals φ_j, (4.20) leads to

$$\frac{\delta E_{\text{total}}}{\delta\Gamma^{(1)}(\mathbf{x};\mathbf{x}')} = \mu\delta(\mathbf{x}-\mathbf{x}') + \sum_{j=1}^{\infty}\frac{\delta F}{\delta n_j}\frac{\delta n_j}{\delta\Gamma^{(1)}(\mathbf{x};\mathbf{x}')} + \sum_{j=1}^{\infty}\int d\mathbf{y}\,\frac{\delta F}{\delta\varphi_j(\mathbf{y})}\frac{\delta\varphi_j(\mathbf{y})}{\delta\Gamma^{(1)}(\mathbf{x};\mathbf{x}')} + c.c. \tag{4.21}$$

At the energy minimum, $\delta F/\delta\varphi_j = 0$ for all natural orbitals and $\delta F/\delta n_l = 0$ for any unpinned state l. The pinned states, however, contribute so that

$$\frac{\delta E_{\text{total}}}{\delta\Gamma^{(1)}(\mathbf{x};\mathbf{x}')}\bigg|_{\min} = \mu\delta(\mathbf{x}-\mathbf{x}') + \sum_p \frac{\delta F}{\delta n_p}\varphi_p^*(\mathbf{x})\varphi_p(\mathbf{x}'), \tag{4.22}$$

where we have used Eq. (2.51). The sum now runs over pinned states only. Equation (4.19) reduces to

$$\begin{aligned} &E_{\text{total}}(M+\eta) - E_{\text{total}}(M) = \\ &\quad \mu(M)\eta + \sum_p \frac{\delta F}{\delta n_p^M}\iint d\mathbf{x}d\mathbf{x}'\,\varphi_p^{*M}(\mathbf{x})\varphi_p^M(\mathbf{x}')\left(\Gamma^{(1)M+\eta}(\mathbf{x};\mathbf{x}') - \Gamma^{(1)M}(\mathbf{x};\mathbf{x}')\right), \end{aligned} \tag{4.23}$$

where the upper index M denotes that the natural orbitals and occupation numbers corresponding to the M-particle density matrix. If we write the occupation numbers and orbitals of the $M+\eta$ system as

$$n_j^{M+\eta} = n_j^M + \delta n_j, \quad \varphi_j^{M+\eta} = \varphi_j^M + \delta\varphi_j, \tag{4.24}$$

all first order corrections to $\Gamma^{(1)M+\eta}$ are contained in

$$\Gamma^{(1)M+\eta}(\mathbf{x};\mathbf{x}') = \sum_{j=1}^{\infty}(n_j^M + \delta n_j)\,(\varphi_j^{M*}(\mathbf{x}') + \delta\varphi_j^*(\mathbf{x}'))\,(\varphi_j^M(\mathbf{x}) + \delta\varphi_j(\mathbf{x}))\,. \quad (4.25)$$

Using the orthonormality of the natural orbitals, this leads to

$$\begin{aligned} &E_{\text{total}}(M+\eta) - E_{\text{total}}(M) = \quad (4.26)\\ &\mu(M)\eta + \sum_p \frac{\delta F}{\delta n_p^M}\left[\delta n_p + n_p^M \int d\mathbf{x}\left(\varphi_p^M(\mathbf{x})\delta\varphi_p^*(\mathbf{x}) + \delta\varphi_p(\mathbf{x})\varphi_p^{*M}(\mathbf{x})\right)\right]. \end{aligned}$$

The second term in the square brackets is zero since the norm of the natural orbitals does not change when the particle number is increased. Hence, $\delta\varphi_p$ is orthogonal to the corresponding φ_p^M. Concerning the first term we observe that the sum is only running over pinned states, i.e. states where the true minimum is at a finite distance from the border of the interval $[0;1]$. Adding an infinitesimal amount of particles η to the system can not unpin these states and, hence, δn_p is zero in the limit $\eta \to 0$. This proves Eq. (4.17), and hence, by (4.15), we can evaluate the fundamental gap from the discontinuity of the Lagrange multiplier $\mu(M)$

$$\Delta = \lim_{\eta\to 0}\left[\mu(M+\eta) - \mu(M-\eta)\right]. \quad (4.27)$$

4.2 N-Representability for Fractional Particle Number

The N-representability conditions for systems with integer particle numbers are discussed in Chapter 2. The proof of Coleman [47] is given in Appendix A. Since this proof is only concerned with integer number of particles we have to extend it to one-body reduced density matrices for $M = N + \eta$ particles, $0 < \eta < 1$, $N \in \mathbb{N}$. In this section we show that the conditions (2.20) and (2.21)

$$0 \le n_j \le 1, \quad \sum_{j=1}^{\infty} n_j = M \quad (4.28)$$

are also valid for fractional particle number.

We call a density matrix of a system with fractional particle number N-representable if it belongs to the set $\mathcal{S}_1$ given by

$$\begin{aligned} \mathcal{S}_1 \;=\; \Big\{ &\Gamma^{(1)M}(\mathbf{x};\mathbf{x}') = (1-\eta)\Gamma^{(1)N}(\mathbf{x};\mathbf{x}') + \eta\Gamma^{(1)N+1}(\mathbf{x};\mathbf{x}'),\\ &\text{with } \Gamma^{(1)N}(\mathbf{x};\mathbf{x}'), \Gamma^{(1)N+1}(\mathbf{x};\mathbf{x}') \text{ ensemble } N-\text{representable}\Big\}. \quad (4.29) \end{aligned}$$

In other words, a density matrix for fractional particle number is N-representable if it can be written as an ensemble of density matrices for integer particle number which are N-representable. We introduce a second set $\mathcal{S}_2$

$$\mathcal{S}_2 = \left\{ \Gamma^{(1)M}(\mathbf{x};\mathbf{x}') = \sum_{j=1}^{\infty} \alpha_j \phi_j^*(\mathbf{x}')\phi_j(\mathbf{x}),\ 0 \leq \alpha_j \leq 1\ \forall j,\ \sum_{j=1}^{\infty} \alpha_j = N + \eta \right\}. \quad (4.30)$$

In order to prove that the conditions (4.28) are necessary and sufficient, we have to show that the two sets $\mathcal{S}_1$ and $\mathcal{S}_2$ are identical.

In the first part of the proof we show that $\mathcal{S}_1 \subseteq \mathcal{S}_2$, i.e. that (4.28) are necessary conditions. Starting from

$$\Gamma^{(1)M}(\mathbf{x};\mathbf{x}') = (1-\eta)\Gamma^{(1)N}(\mathbf{x};\mathbf{x}') + \eta\Gamma^{(1)N+1}(\mathbf{x};\mathbf{x}') \quad (4.31)$$

we diagonalize $\Gamma^{(1)M}$ and obtain, due to its hermiticity,

$$\Gamma^{(1)M}(\mathbf{x};\mathbf{x}') = \sum_{j=1}^{\infty} n_j^M \varphi_j^{M*}(\mathbf{x}')\varphi_j^M(\mathbf{x}), \quad (4.32)$$

where n_j^M and φ_j^M denote the eigenvalues and eigenfunctions of $\Gamma^{(1)M}$, respectively. We also diagonalize $\Gamma^{(1)N}$ and $\Gamma^{(1)N+1}$ and, since they are both N-representable, we obtain

$$\Gamma^{(1)N}(\mathbf{x};\mathbf{x}') = \sum_{j=1}^{\infty} n_j^N \varphi_j^{N*}(\mathbf{x}')\varphi_j^N(\mathbf{x}) , \quad (4.33)$$

$$\Gamma^{(1)N+1}(\mathbf{x};\mathbf{x}') = \sum_{j=1}^{\infty} n_j^{N+1} \varphi_j^{N+1*}(\mathbf{x}')\varphi_j^{N+1}(\mathbf{x}) \quad (4.34)$$

with

$$0 \leq n_j^N \leq 1, \qquad \sum_{j=1}^{\infty} n_j^N = N, \quad (4.35)$$

$$0 \leq n_j^{N+1} \leq 1, \qquad \sum_{j=1}^{\infty} n_j^{N+1} = N+1. \quad (4.36)$$

In order to compare (4.31) and (4.32) we expand the natural orbitals of $\Gamma^{(1)N}$ and $\Gamma^{(1)N+1}$ in the natural orbitals of $\Gamma^{(1)M}$, i.e.

$$\varphi_j^N(\mathbf{x}) = \sum_{k=1}^{\infty} c_{jk}^N \varphi_k^M(\mathbf{x}), \quad (4.37)$$

$$\varphi_j^{N+1}(\mathbf{x}) = \sum_{k=1}^{\infty} c_{jk}^{N+1} \varphi_k^M(\mathbf{x}). \quad (4.38)$$

Such an expansion is always possible since the natural orbitals of a density matrix form a complete orthonormal set of functions. We can then rewrite (4.31) as

$$\begin{aligned}\Gamma^{(1)M}(\mathbf{x};\mathbf{x}') &= (1-\eta)\sum_{j,k,l=1}^{\infty} n_j^N c_{jk}^{N*} c_{jl}^N \varphi_k^{M*}(\mathbf{x}')\varphi_l^M(\mathbf{x}) \\ &\quad +\eta\sum_{j,k,l=1}^{\infty} n_j^{N+1} c_{jk}^{N+1*} c_{jl}^{N+1} \varphi_k^{M*}(\mathbf{x}')\varphi_l^M(\mathbf{x}) \qquad (4.39)\\ &= \sum_{k=1}^{\infty} n_k^M \varphi_k^{M*}(\mathbf{x}')\varphi_k^M(\mathbf{x}). \qquad (4.40)\end{aligned}$$

A comparison of the coefficients shows that all terms with $k \neq l$ in the first two sums have to vanish and, furthermore, we obtain

$$n_k^M = (1-\eta)\sum_{j=1}^{\infty} n_j^N \mid c_{jk}^N \mid^2 +\eta\sum_{j=1}^{\infty} n_j^{N+1} \mid c_{jk}^{N+1} \mid^2 . \qquad (4.41)$$

From the normalization of the three sets of natural orbitals, φ_j^N, φ_j^{N+1}, and φ_j^M, we know that the expansion coefficients satisfy

$$\sum_{j=1}^{\infty} \mid c_{jk}^N \mid^2 = \sum_{j=1}^{\infty} \mid c_{jk}^{N+1} \mid^2 = 1. \qquad (4.42)$$

As a result we conclude

$$\begin{aligned} 0 \leq & \quad \textstyle\sum_{j=1}^{\infty} n_j^N \mid c_{jk}^N \mid^2 \quad \leq 1 \,, & (4.43)\\ 0 \leq & \quad \textstyle\sum_{j=1}^{\infty} n_j^{N+1} \mid c_{jk}^{N+1} \mid^2 \quad \leq 1 & (4.44)\end{aligned}$$

because the occupation numbers n_j^N and n_j^{N+1} are between zero and one and hence the sums are reduced compared to those in Eq. (4.42). Multiplying Eqs. (4.43) and (4.44) with $1-\eta$ and η, respectively, leads to

$$\begin{aligned} 0 \leq & \quad (1-\eta)\textstyle\sum_{j=1}^{\infty} n_j^N \mid c_{jk}^N \mid^2 \quad \leq 1-\eta & (4.45)\\ 0 \leq & \quad \eta\textstyle\sum_{j=1}^{\infty} n_j^{N+1} \mid c_{jk}^{N+1} \mid^2 \quad \leq \eta & (4.46)\end{aligned}$$

which shows together with (4.41) that indeed

$$0 \leq n_k^M \leq 1. \qquad (4.47)$$

It is straightforward to show that $\sum_k n_k^M = M = N + \eta$ by using (4.41), (4.42) with $\sum_j$ replaced by $\sum_k$, and the constraints for n_j^N and n_j^{N+1}. Therefore, we have shown $\mathcal{S}_1 \subseteq \mathcal{S}_2$.

In the second part we have to prove $\mathcal{S}_2 \subseteq \mathcal{S}_1$, i.e. that the conditions (4.28) are also sufficient. We use some of the theorems and methods already employed

by Coleman in his proof of the N-representability for integer particle number [47]. First, we show that the two sets are convex (see also App. A). The weighted average of two elements $\Gamma_1^{(1)M}$ and $\Gamma_2^{(1)M}$ of $\mathcal{S}_1$ is given by

$$\begin{aligned}\Gamma_3^{(1)M} &= \alpha\Gamma_1^{(1)M} + (1-\alpha)\Gamma_2^{(1)M} \\ &= \alpha\left[(1-\eta)\Gamma_1^{(1)N} + \eta\Gamma_1^{(1)N+1}\right] + (1-\alpha)\left[(1-\eta)\Gamma_2^{(1)N} + \eta\Gamma_2^{(1)N+1}\right] \\ &= (1-\eta)\left[\alpha\Gamma_1^{(1)N} + (1-\alpha)\Gamma_2^{(1)N}\right] + \eta\left[\alpha\Gamma_1^{(1)N+1} + (1-\alpha)\Gamma_2^{(1)N+1}\right] \\ &= (1-\eta)\Gamma_3^{(1)N} + \eta\Gamma_3^{(1)N+1}. \end{aligned} \tag{4.48}$$

Due to the convexity of the sets of N-representable density matrices for integer particle number, $\Gamma_3^{(1)N}$ and $\Gamma_3^{(1)N+1}$ are N-representable and therefore $\Gamma_3^{(1)M}$ is also an element of $\mathcal{S}_1$ which proves the convexity of this set.

In order to show that $\mathcal{S}_2$ is convex we employ a theorem from linear algebra: The maximum eigenvalue of the sum of two positive definite operators is smaller or at most equal to the sum of the maximum eigenvalues of the two operators. For a weighted average of two elements of $\mathcal{S}_2$, $\Gamma_1^{(1)M}$ and $\Gamma_2^{(1)M}$, we add the operators $\alpha\Gamma_1^{(1)M}$ and $(1-\alpha)\Gamma_2^{(1)M}$ having maximum eigenvalues α and $1-\alpha$, respectively. The maximum eigenvalue of

$$\Gamma_3^{(1)M} = \alpha\Gamma_1^{(1)M} + (1-\alpha)\Gamma_2^{(1)M} \tag{4.49}$$

is hence 1. Since the sum of two positive definite operators is again a positive definite operator, $\Gamma_3^{(1)M}$ has no negative eigenvalues. Therefore, all eigenvalues of $\Gamma_3^{(1)M}$ are elements of $[0;1]$ so that $\Gamma_3^{(1)M}$ is an element of $\mathcal{S}_2$ which is hence a convex set.

Due to the Krein-Milman theorem [48] any convex set is completely defined by its extreme elements. Therefore, we show next that the extreme elements of $\mathcal{S}_2$ are those density matrices $\Gamma_e^{(1)M}$ with exactly N occupation numbers equal to one and one occupation number equal to η, i.e.

$$\Gamma_e^{(1)M}(\mathbf{x};\mathbf{x}') = \sum_{j=1}^{N+1} n_j \varphi_j^*(\mathbf{x}')\varphi_j(\mathbf{x}), \quad \begin{cases} n_j = 1 & j \leq N \\ n_j = \eta & j = N+1 \\ n_j = 0 & j > N+1. \end{cases} \tag{4.50}$$

First, we show that these elements are indeed extreme which means that they can not be written as the weighted average of two other elements of $\mathcal{S}_2$. Then we prove that there are no other extreme elements. Since the proof of the first step is by contradiction, we assume that $\Gamma_e^{(1)M}$ can be written as

$$\Gamma_e^{(1)M} = \alpha\Gamma_1^{(1)M} + (1-\alpha)\Gamma_2^{(1)M}, \tag{4.51}$$

with $\Gamma_1^{(1)M}, \Gamma_2^{(1)M} \in \mathcal{S}_2$ and $0 < \alpha < 1$. For the rank R of the extreme element (i.e. the number of non-zero eigenvalues) one has $R = N+1$ while $R \geq N+1$ for any element of $\mathcal{S}_2$. The rank of a positive definite operator is equal to the dimension of

its range. The range of the sum of two positive definite operators is equal to the union of their ranges. Hence, if the sum of two density matrices is to have rank $N+1$, both density matrices must have rank $N+1$. Since $R = N+1$ for $\Gamma_e^{(1)M}$ in Eq. (4.51) both $\Gamma_1^{(1)M}$ and $\Gamma_2^{(1)M}$ have to have $N+1$ non-zero eigenvalues and their ranges are both identical to the range of $\Gamma_e^{(1)M}$. We can therefore expand the natural orbitals of $\Gamma_1^{(1)M}$ and $\Gamma_2^{(1)M}$ in the natural orbitals of $\Gamma_e^{(1)M}$ according to

$$\varphi_{k1}(\mathbf{r}) = \sum_{j=1}^{N+1} c_{jk1}\, \varphi_j(\mathbf{r}), \tag{4.52}$$

$$\varphi_{k2}(\mathbf{r}) = \sum_{j=1}^{N+1} c_{jk2}\, \varphi_j(\mathbf{r}). \tag{4.53}$$

Using these expansions together with (4.50) and (4.51) yields

$$\sum_{k=1}^{N+1} \alpha\, n_{j1} \mid c_{jk1} \mid^2 + (1-\alpha)\, n_{j2} \mid c_{jk2} \mid^2 = 1, \quad j = 1...N. \tag{4.54}$$

Due to the normalization of the expansion coefficients and the properties of the occupation numbers this equation can only be satisfied if the fully occupied orbitals $\varphi_1 ... \varphi_N$ only contribute to fully occupied orbitals φ_{k1} and φ_{k2}. Therefore, the fully occupied orbitals of the three matrices $\Gamma_e^{(1)M}$, $\Gamma_1^{(1)M}$, and $\Gamma_2^{(1)M}$ span the same N-dimensional space. The $(N+1)^{st}$ orbital of the three matrices is hence identical and has occupation number η in all three cases. In other words, the three matrices are connected by a unitary transformation in the subspace of fully occupied orbitals and therefore identical, i.e. $\Gamma_1^{(1)M} = \Gamma_2^{(1)M} = \Gamma_e^{(1)M}$ which is therefore an extreme element of $\mathcal{S}_2$.

Now, we prove, again by contradiction, that there exist no other extreme elements. Assume there is an extreme element $\Gamma_1^{(1)M}$ which is not of the above kind. Then there are two different possibilities:

(1) $\Gamma_1^{(1)M}$ has more than $N+1$ non-zero eigenvalues.

(2) $\Gamma_1^{(1)M}$ has exactly $N+1$ non-zero eigenvalues but at least one differs from both 1 and η.

In the first case, we order the occupation numbers of $\Gamma_1^{(1)M}$ such that

$$1 \geq n_{1,1}^M \geq n_{1,2}^M \geq ... \geq n_{1,N}^M \geq n_{1,N+1}^M \geq n_{1,N+2}^M \geq ... \geq 0. \tag{4.55}$$

In addition, one has $n_{1,N+1}^M < 1$ and $n_{1,N+2}^M > 0$. The first index implies that these occupation numbers belong to $\Gamma_1^{(1)M}$. We can then always find an ϵ, $0 < \epsilon < 1$ such that

$$\begin{array}{rll} & n_{1i}^M \geq \epsilon & i = 1...N\,, \\ 1-\epsilon \geq & n_{1i}^M \geq \eta\epsilon & i = N+1\,, \\ 1-\epsilon \geq & n_{1i}^M & i \geq N+2\,. \end{array} \tag{4.56}$$

We decompose $\Gamma_1^{(1)M}$ into $\Gamma_e^{(1)M}$ and $\Gamma_2^{(1)M}$ according to

$$\Gamma_1^{(1)M} = \epsilon\Gamma_e^{(1)M} + (1-\epsilon)\Gamma_2^{(1)M}, \tag{4.57}$$

where $\Gamma_e^{(1)M}$ denotes the extreme element with the first N occupation numbers equal to 1 and the $(N+1)^{st}$ equal to η. All three matrices share the same set of natural orbitals. The occupation numbers of $\Gamma_2^{(1)M}$ are therefore given as

$$\begin{array}{rcll} n_{2i}^M &=& (n_{1i}^M - \epsilon)/(1-\epsilon) & i = 1...N, \\ n_{2i}^M &=& (n_{1i}^M - \eta\epsilon)/(1-\epsilon) & i = N+1, \\ n_{2i}^M &=& n_{1i}^M/(1-\epsilon) & i \geq N+2. \end{array} \tag{4.58}$$

Due to the restrictions (4.56), $0 \leq n_{2i}^M \leq 1$ and their sum is equal to M. Hence, $\Gamma_2^{(1)M}$ is an element of $\mathcal{S}_2$. This, however, implies that $\Gamma_1^{(1)M}$ is not an extreme element.

In the second case we can immediately conclude that all $N+1$ non-zero occupation numbers have to be larger than η. Therefore, we can always find an ϵ, $0 < \epsilon < 1$ such that

$$\begin{array}{ll} n_{1i}^M \geq \eta + \epsilon & i = 1...N+1, \\ n_{1i}^M = 0 & i \geq N+2. \end{array} \tag{4.59}$$

As in the first case, we find

$$\Gamma_1^{(1)M} = \epsilon\Gamma_e^{(1)M} + (1-\epsilon)\Gamma_2^{(1)M}, \tag{4.60}$$

where the occupation numbers of $\Gamma_2^{(1)M}$ are now given by

$$\begin{array}{rcll} n_{2i}^M &=& (n_{1i}^M - \epsilon)/(1-\epsilon) & i = 1...N\ , \\ n_{2i}^M &=& (n_{1i}^M - \eta\epsilon)/(1-\epsilon) & i = N+1\ , \\ n_{2i}^M &=& 0 & i \geq N+2\ . \end{array} \tag{4.61}$$

Again, from the restrictions (4.59), all occupation numbers n_{2i}^M are elements of the interval $[0;1]$ and sum up to M. Therefore, $\Gamma_2^{(1)M}$ is an element of $\mathcal{S}_2$ and $\Gamma_1^{(1)M}$ is not extreme. We have therefore proven that an element of $\mathcal{S}_2$ is extreme if and only if it has exactly N eigenvalues equal to 1 and one eigenvalue equal to η.

Due to the convexity of $\mathcal{S}_2$ any of its elements can be written as a weighted average of the extreme elements, i.e.

$$\Gamma^{(1)M} = \sum_{j\in\{e\}} \alpha_j \Gamma_j^{(1)M} \quad \text{with} \quad \sum_j \alpha_j = 1 \quad \forall\Gamma^{(1)M} \in \mathcal{S}_2, \tag{4.62}$$

where the sum runs over all extreme elements. To prove $\mathcal{S}_2 \subseteq \mathcal{S}_1$, it therefore remains to be shown that an arbitrary extreme element of $\mathcal{S}_2$ is also an element of $\mathcal{S}_1$. This is, however, easily done by explicit construction. Writing

$$\Gamma_e^{(1)M} = (1-\eta)\sum_{j=1}^{N} \varphi_j^*(\mathbf{x}')\varphi_j(\mathbf{x}) + \eta\sum_{j=1}^{N+1} \varphi_j^*(\mathbf{x}')\varphi_j(\mathbf{x}), \tag{4.63}$$

where $\varphi_j(\mathbf{x})$ are the natural orbitals of $\Gamma_e^{(1)M}$ the first sum represents a single Slater determinant in N-particle space and the second is a single Slater determinant for $N+1$ particles. Both sums are N-representable density matrices and, hence, the extreme element $\Gamma_e^{(1)M}$ of $\mathcal{S}_2$ is also an element of $\mathcal{S}_1$. As shown above, $\mathcal{S}_1$ is a convex set and, therefore, any weighted average of two of its elements is again an element of the set. Since all elements of $\mathcal{S}_2$ can be written as weighted averages of the extreme elements, this implies $\mathcal{S}_2 \subseteq \mathcal{S}_1$. We have therefore shown that

$$\mathcal{S}_1 \subseteq \mathcal{S}_2 \subseteq \mathcal{S}_1, \tag{4.64}$$

which can only be fulfilled if

$$\mathcal{S}_1 \equiv \mathcal{S}_2. \tag{4.65}$$

Hence, restricting the occupation numbers of $\Gamma^{(1)M}$ according to $\mathcal{S}_2$ is necessary and sufficient to ensure N-representability.

4.3 Numerical Treatment

After settling the issue of N-representability, in this section we consider the actual numerical treatment of finite and periodic systems in RDMFT. We first discuss issues which are independent of the specific system before we focus on a more specific description of finite and periodic systems.

The normalization of the density matrix and the orthonormality of the natural orbitals are realized by adding Lagrange multipliers to the total energy functional. Hence, we minimize

$$F[\Gamma^{(1)}] = E_{\text{total}}[\Gamma^{(1)}] - \mu\left(\sum_{j=1}^{\infty} n_j - N\right) - \sum_{j,k=1}^{\infty} \epsilon_{jk}\left(\int d\mathbf{x}\, \varphi_j^*(\mathbf{x})\varphi_k(\mathbf{x}) - \delta_{jk}\right). \tag{4.66}$$

As discussed already in Section 2.5, the additional N-representability constraint $0 \leq n_j \leq 1$ is enforced by the substitution $n_j = \sin^2\theta_j$.

The natural orbitals are expanded in an appropriate basis set. The minimization is therefore equivalent to finding the optimal expansion coefficients for each natural orbital. The minimization of Eq. (4.66) with respect to the natural orbitals, i.e. taking the functional derivative of (4.66) with respect to orbital j and setting it to zero, leads to equations of the form

$$\mathcal{F}^{(j)}\varphi_j = \sum_{k=1}^{\infty} \epsilon_{jk}\,\varphi_k, \tag{4.67}$$

$$\epsilon_{jk} = \epsilon_{kj}, \tag{4.68}$$

where $\mathcal{F}^{(j)}$ is an orbital-dependent operator, i.e. it depends on the orbital φ_j it acts on. As a consequence, the Lagrange multipliers ϵ_{jk} are non-diagonal. For an

orbital independent operator $\mathcal{F}$ the orthogonality of the eigenfunctions is automatically satisfied and only the normalization is enforced by a then diagonal Lagrange multiplier. Orbital-dependent operators, however, are not unusual, they also appear in DFT calculations when self-interaction corrected LDA functionals are used or in restricted open-shell Hartree-Fock calculations.

Differentiating with respect to the occupation numbers, we obtain

$$\frac{\delta F}{\delta \theta_j} = 2 \sin\theta_j \cos\theta_j \left[\frac{\delta E_{\text{total}}}{\delta n_j} - \mu \right] = 0, \tag{4.69}$$

which has two different types of solutions. For the pinned states the occupation numbers n_j are either zero or one and therefore $\sin\theta_j$ or $\cos\theta_j$ is zero. For states with fractional occupation numbers

$$\frac{\delta E_{\text{total}}}{\delta n_j} = \mu \tag{4.70}$$

has to be satisfied.

In principle, one has to solve the system of equations consisting of (4.67), (4.68), and (4.69) plus the additional constraints from the Lagrange multipliers. Since these equations are generally non-linear a direct solution is very demanding. Therefore, one finds a minimum of the functional (4.66) employing a conjugate gradient scheme. Eqs. (4.67), (4.68), and (4.69) then determine the gradient in each iteration. For the initial guess we use the results of a Hartree-Fock calculation which should be sufficiently close to the minimum of the functional (4.66). One should be aware that the conjugate gradient scheme does not guarantee that the absolute minimum is found. The minimization is implemented as a two-step process. In each iteration we first find the optimal set of occupation numbers from (4.69) using the orbitals from the previous iteration. Then these occupation numbers are kept fixed and a new set of orbitals is obtained from (4.67) and (4.68). The orbitals are orthogonalized in each iteration. The whole process is iterated until it converges. In an outer loop, the chemical potential μ is adjusted to satisfy the particle number constraint.

4.3.1 Finite Open- and Closed-Shell Systems

In principle, open- and closed-shell systems can be treated on the same footing. In practice, however, one can use spin independent natural orbitals in the case of closed-shell systems which can then be doubly occupied. This simplifies the numerical treatment significantly. The total energy for a closed-shell system employing the Goedecker/Umrigar approximation (see Section 3.3) for the exchange-correlation energy reads

$$E_{\text{total}}^{GU} = \sum_{j=1}^{\infty} n_j h_{jj} + \sum_{j,k=1}^{\infty} n_j n_k (2 - \delta_{jk}) J_{jk} - \sum_{j,k=1}^{\infty} \sqrt{n_j n_k} (1 - \delta_{jk}) K_{jk}. \tag{4.71}$$

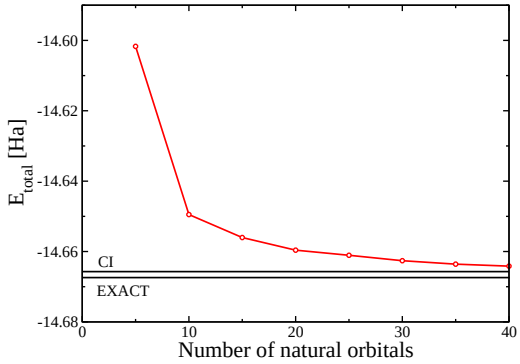

Figure 4.3: The total energy of Beryllium atom in the singlet state as a function of the natural orbitals for the Goedecker/Umrigar functional. For comparison the CI and exact values [49, 50] are also shown.

The one-body integral h_{jj} is given by

$$h_{jj} = \iint d\mathbf{r}d\mathbf{r}' \, \varphi_j^*(\mathbf{r}') \left(\delta(\mathbf{r}-\mathbf{r}') \left(-\frac{\nabla^2}{2} \right) + v_0(\mathbf{r}', \mathbf{r}) \right) \varphi_j(\mathbf{r}) \, , \tag{4.72}$$

and the two-body integrals, Coulomb and exchange respectively, read

$$J_{jk} = \iint d\mathbf{r}d\mathbf{r}' \, \frac{\varphi_j(\mathbf{r})\varphi_j^*(\mathbf{r})\varphi_k(\mathbf{r}')\varphi_k^*(\mathbf{r}')}{\mid \mathbf{r}-\mathbf{r}' \mid} \, , \tag{4.73}$$

$$K_{jk} = \iint d\mathbf{r}d\mathbf{r}' \, \frac{\varphi_j(\mathbf{r})\varphi_j^*(\mathbf{r}')\varphi_k(\mathbf{r}')\varphi_k^*(\mathbf{r})}{\mid \mathbf{r}-\mathbf{r}' \mid} \, . \tag{4.74}$$

We employ the GAMESS computer code [51] to calculate both the one-body as well as the two-body integrals. The GAMESS code is also used to obtain the Hartree-Fock solution which we use as a starting point for the RDMFT calculation. The natural orbitals are expanded in a Gaussian type basis set (cc-PVQZ [36]) which contains between 30 and 100 basis functions depending on the chemical element. This immediately leads to the question of how many natural orbitals have to be taken into account in the calculation to reach a satisfying accuracy. In principle, all sums run over infinitely many natural orbitals. However, only a finite number of occupation numbers is significantly larger than zero and the sums can be safely truncated. Before truncating we have to ensure that the results are well converged with respect to the number of natural orbitals taken into account. Fig. 4.3 shows the convergence of the total energy as a function of the number of natural orbitals for the Beryllium atom in its singlet ground state for the Goedecker/Umrigar functional. As one can see, the inclusion of 20 natural orbitals yields an accuracy of 0.01 Ha for the total energy. Including 40 natural orbitals one reaches the same accuracy as the CI calculation. All higher orbitals have such a small occupation that their inclusion does not significantly influence the results.

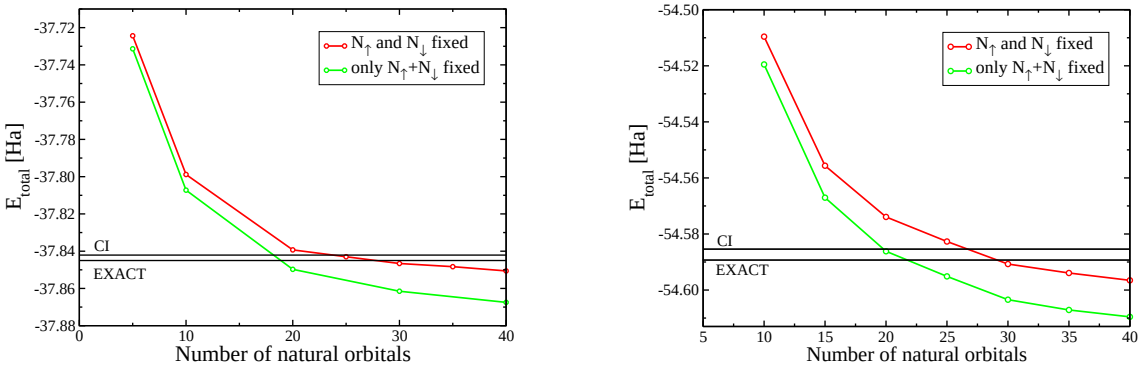

Figure 4.4: The total energy of the Carbon triplet state (left) and the Nitrogen quartet state (right) as a function of the number of natural orbitals for the restricted open-shell version of the Goedecker/Umrigar functional. For comparison, the CI and the exact values [49, 50] are also given.

For open-shell systems the formalism based on spin-independent orbitals is obviously no longer valid. Not considering the full spinor treatment, one at least has to use spin dependent occupation numbers and orbitals. The resulting states are, as discussed in Section 2.6, no longer eigenfunctions of the total spin operator $\mathbf{S}^2$ [52]. In our treatment we prefer to keep eigenstates of the total spin operator and therefore use a method in analogy to restricted open-shell Hartree-Fock, which we call restricted open-shell RDMFT. In this formalism the occupation numbers are spin dependent while the natural orbitals remain spin independent. The Goedecker/Umrigar functional is then given by

$$\begin{aligned} E_{\text{total}}^{GU} &= \sum_{j=1}^{\infty} \left(n_j^{\uparrow} + n_j^{\downarrow}\right) h_{jj} \\ &+ \frac{1}{2} \sum_{j,k=1}^{\infty} \left[\left(n_j^{\uparrow} n_k^{\uparrow} + n_j^{\downarrow} n_k^{\downarrow}\right)(1-\delta_{jk}) + \left(n_j^{\uparrow} n_k^{\downarrow} + n_j^{\downarrow} n_k^{\uparrow}\right)\right] J_{jk} \\ &- \frac{1}{2} \sum_{j,k=1}^{\infty} \left[\left(\sqrt{n_j^{\uparrow} n_k^{\uparrow}} + \sqrt{n_j^{\downarrow} n_k^{\downarrow}}\right)(1-\delta_{jk})\right] K_{jk}. \end{aligned} \tag{4.75}$$

The one-body integral h_{jj} and the two-body integrals J_{jk} and K_{jk} are again given by Eqs. (4.72)-(4.74).

As a consequence of the spin-dependent occupation numbers, there are two different ways to implement the constraint of particle number conservation. We can either use a single Lagrange multiplier μ which fixes the total number of particles as for the closed-shell system, or we use a spin resolved constraint, i.e. $\mu^{\uparrow}$ and $\mu^{\downarrow}$ fixing the number of spin-up and spin-down electrons separately. In the first case there is the possibility of charge diffusion between the different spin channels and the total

Atom	RDMFT		QCI	Exact
	$\mu^{\uparrow} = \mu^{\downarrow}$	$\mu^{\downarrow} \neq \mu^{\uparrow}$		
Li	7.4940	7.4827	7.4743	7.4781
B	24.6746	24.6616	24.6515	24.6539
C	37.8675	37.8506	37.8421	37.8450
N	54.6096	54.5965	54.5854	54.5893
O	75.0668	75.0671	75.0613	75.0670
F	99.6951	99.6952	99.727	99.734
$\bar{\Delta}$	0.020	0.010	0.004	0.000

Table 4.1: Total energies for the first-row open-shell atoms (in Ha) for the restricted open-shell Goedecker/Umrigar functional with and without enforcing the spin conservation constraint. The QCI and exact values [49, 50] are given for comparison. $\bar{\Delta}$ denotes the mean absolute deviation from the exact values.

spin in z-direction is not fixed. The spin resolved Lagrange multipliers, on the other hand, fix the total spin. Fig. 4.4 compares the two methods for a Carbon atom in the triplet state and the Nitrogen quartet state. In comparison with the exact value the spin-dependent μ is superior to a spin independent treatment in both cases. Due to the approximative nature of the energy functional the total energy is smaller than the exact value independent of the spin treatment. The results are again well converged for about 40 orbitals.

For finite systems, open- as well as closed-shell, the inclusion of 20 to 50 natural orbitals for the considered atomic species is sufficient to obtain well converged results. The number of needed orbitals is, of course, expected to increase with increasing system size. Hence, for all systems considered in this thesis an investigation of the convergence precedes all other calculations.

Calculating the total energies of the first row open-shell atoms with the two different choices for the Lagrange multiplier, the spin-dependent treatment is again superior, see Table 4.1. The average error, compared to the exact results, is a factor of two smaller compared to the, already quite good, results of the spin-independent treatment. Therefore, a spin-dependent μ is used in all following calculations for open-shell systems.

4.3.2 Periodic Systems

Periodic systems are commonly employed in the description of solids. While this is, of course, not expected to capture any effects arising from the surface it yields a very accurate description of bulk properties. Bloch's theorem, a consequence of the periodicity of the lattice and the corresponding discrete translational invariance, requires the natural orbitals to be Bloch states, i.e.

$$\varphi_{\alpha\mathbf{k}}(\mathbf{r} + \mathbf{R}) = \exp(i\mathbf{k}\mathbf{R})\varphi_{\alpha\mathbf{k}}(\mathbf{r}), \tag{4.76}$$

for any lattice vector $\mathbf{R}$. The orbitals are labelled with a band index α and a wave vector $\mathbf{k}$ restricted to the first Brillouin zone. Since the Bloch wave functions are delocalized over the whole crystal the evaluation of the one- and two-body integrals using Bloch orbitals is very demanding. Alternatively, one can use Wannier functions which are also orthonormal but localized. They form a complete set of functions spanning the same space as the Bloch orbitals. The connection between Bloch and Wannier states is given by the Wannier transformation

$$\Phi_\alpha(\mathbf{r}-\mathbf{R}) = \sum_{\mathbf{k}} \exp(-i\mathbf{k}(\mathbf{r}-\mathbf{R}))\varphi_{\alpha\mathbf{k}}(\mathbf{r}). \tag{4.77}$$

The resulting Wannier functions $\Phi_\alpha(\mathbf{r}-\mathbf{R})$ are centred at lattice position $\mathbf{R}$ and carry the same band index as the original Bloch states. Identical copies of the Wannier states are used throughout the entire crystal due to the periodicity of the lattice. The 1-RDM of a periodic system can hence be written as

$$\begin{aligned}\Gamma^{(1)}(\mathbf{r};\mathbf{r}') &= \sum_{\alpha\mathbf{k}} n_{\alpha\mathbf{k}}\, \varphi^*_{\alpha\mathbf{k}}(\mathbf{r}')\, \varphi_{\alpha\mathbf{k}}(\mathbf{r}) &(4.78)\\ &= \sum_{\mathbf{R},\mathbf{R}'} \sum_{\alpha\mathbf{k}} n_{\alpha\mathbf{k}}\, \exp(i\mathbf{k}(\mathbf{R}-\mathbf{R}')\, \Phi^*_\alpha(\mathbf{r}'+\mathbf{R}')\, \Phi_\alpha(\mathbf{r}+\mathbf{R}). &(4.79)\end{aligned}$$

For $\mathbf{k}$-independent occupation numbers $n_{\alpha\mathbf{k}}$, which one finds in the HF calculation of semiconductors and insulators, the $\mathbf{k}$ summation yields a Delta-function in $\mathbf{R}$ and $\mathbf{R}'$ and the 1-RDM reduces to

$$\Gamma^{(1)}(\mathbf{r};\mathbf{r}') = \sum_{\mathbf{R}} \sum_{\alpha} n_\alpha \Phi^*_\alpha(\mathbf{r}'+\mathbf{R})\Phi_\alpha(\mathbf{r}+\mathbf{R}). \tag{4.80}$$

In other words, the natural orbitals can also be written as Wannier functions. However, in RDMFT the occupation numbers are, in general, $\mathbf{k}$-dependent. Writing the 1-RDM in terms of Wannier functions is therefore approximative. Alternatively, the use of Wannier states can be regarded as a different approximation for the exchange-correlation energy. Using the same functional form with Wannier or Bloch states always yields two fundamentally different approximations due to the fractional nature of the occupation numbers which implies a $\mathbf{k}$-dependence. Of course, the quality of the Wannier functional needs to be tested. Intuitively, one would expect a reasonable description for systems with flat bands, i.e. strong localization like in ionic solids. As an additional advantage, the occupation numbers, using Wannier orbitals, are wave vector independent leading to a simpler RDMFT functional. Moreover, because of the localized nature of the Wannier orbitals all calculations can be performed for a single central unit cell. The energy per unit cell for the Goedecker/Umrigar functional is given by (for closed-shell systems)

$$\frac{E}{N_{\mathrm{uc}}} = 2\sum_{\alpha} n_\alpha h_{0\alpha} + \sum_{\alpha,\beta} n_\alpha n_\beta J_{\alpha\beta} - \sum_{\alpha,\beta} \sqrt{n_\alpha n_\beta} K_{\alpha\beta} + E_{\mathrm{nuc}}, \tag{4.81}$$

where $N_{\rm uc}$ denotes the number of unit cells. Due to the periodicity of the lattice it is sufficient to evaluate the one- and two-body integrals at $\mathbf{R} = 0$. They are therefore given by

$$h_{0\alpha} = \iint d\mathbf{r}d\mathbf{r}'\, \Phi^*_\alpha(\mathbf{r}') \left[\delta(\mathbf{r}-\mathbf{r}') \left(-\frac{\nabla^2}{2}\right) + v_0(\mathbf{r},\mathbf{r}')\right] \Phi_\alpha(\mathbf{r})\ , \tag{4.82}$$

$$J_{\alpha\beta} = \sum_{\mathbf{R}'} (2 - \delta_{\alpha\beta}\delta_{\mathbf{R}'0}) \iint d\mathbf{r}d\mathbf{r}'\, \frac{\Phi^*_\alpha(\mathbf{r}-\mathbf{R}')\Phi_\beta(\mathbf{r}')\Phi^*_\beta(\mathbf{r}')\Phi_\alpha(\mathbf{r}-\mathbf{R}')}{\mid \mathbf{r}-\mathbf{r}' \mid}\ , \tag{4.83}$$

$$K_{\alpha\beta} = \sum_{\mathbf{R}'} (1 - \delta_{\alpha\beta}\delta_{\mathbf{R}'0}) \iint d\mathbf{r}d\mathbf{r}'\, \frac{\Phi^*_\alpha(\mathbf{r}-\mathbf{R}')\Phi_\beta(\mathbf{r})\Phi^*_\beta(\mathbf{r}'+\mathbf{R}')\Phi_\alpha(\mathbf{r}')}{\mid \mathbf{r}-\mathbf{r}' \mid}\ . \tag{4.84}$$

The contribution to the total energy from the repulsion of the nuclei reads

$$E_{\rm nuc} = \frac{1}{2} {\sum_{j,k}}' \sum_{\mathbf{R}'} \frac{Z_j Z_k}{\mid \mathbf{R}' + \mathbf{r}_j - \mathbf{r}_k \mid}, \tag{4.85}$$

where $\mathbf{r}_j + \mathbf{R}'$ and $\mathbf{r}_k$ denote the positions of ions with charge Z_j and Z_k, respectively, and the prime on the first sum implies that no ion interacts with itself. In order to determine the Wannier orbitals directly by a variational procedure it is necessary to impose a localization constraint. This can be accomplished by introducing a penalty factor proportional to the overlap of an orbital localized at the reference lattice site with all the basis-set orbitals outside a locally prescribed environment [53, 54] around the reference site. An implementation of this procedure is available in the WANNIER computer code [53, 54]. Our Wannier RDMFT calculation for periodic systems is implemented on top of the WANNIER code. The latter is used to evaluate the integrals over the basis functions, for the HF calculations determining the initial values, and for performing the lattice summations.

As a first application we consider the ionic LiH chain being a good candidate for localized natural orbitals. We use a Gaussian type basis set [59] which allows us to occupy up to 10 natural orbitals in the minimization procedure.

At first sight the functional (4.81) seems to be pathologic due to the non-convergent behaviour of the different contributions with respect to the lattice summation. In an actual calculation, the number of lattice sites on each side of the reference cell is given by the lattice cut-off parameter l_c. Examining the stability of the functional with respect to l_c reveals that the quantities of interest, occupation numbers and the correlation energy, quickly converge, see Fig. 4.5. Fig. 4.5 also shows that the one-electron energy, i.e. the contribution from the one-body integrals, being a non-convergent lattice sum depends dramatically on the cut-off parameter. However, for the quantities of interest we can conclude that $l_c = 50$ is sufficient to obtain accurate results.

Table 4.2 shows a comparison of the total energy of the LiH chain calculated from RDMFT and a variety of different electronic structure methods. Apart from the first two results and the RDMFT calculation which use Wannier-type orbitals,

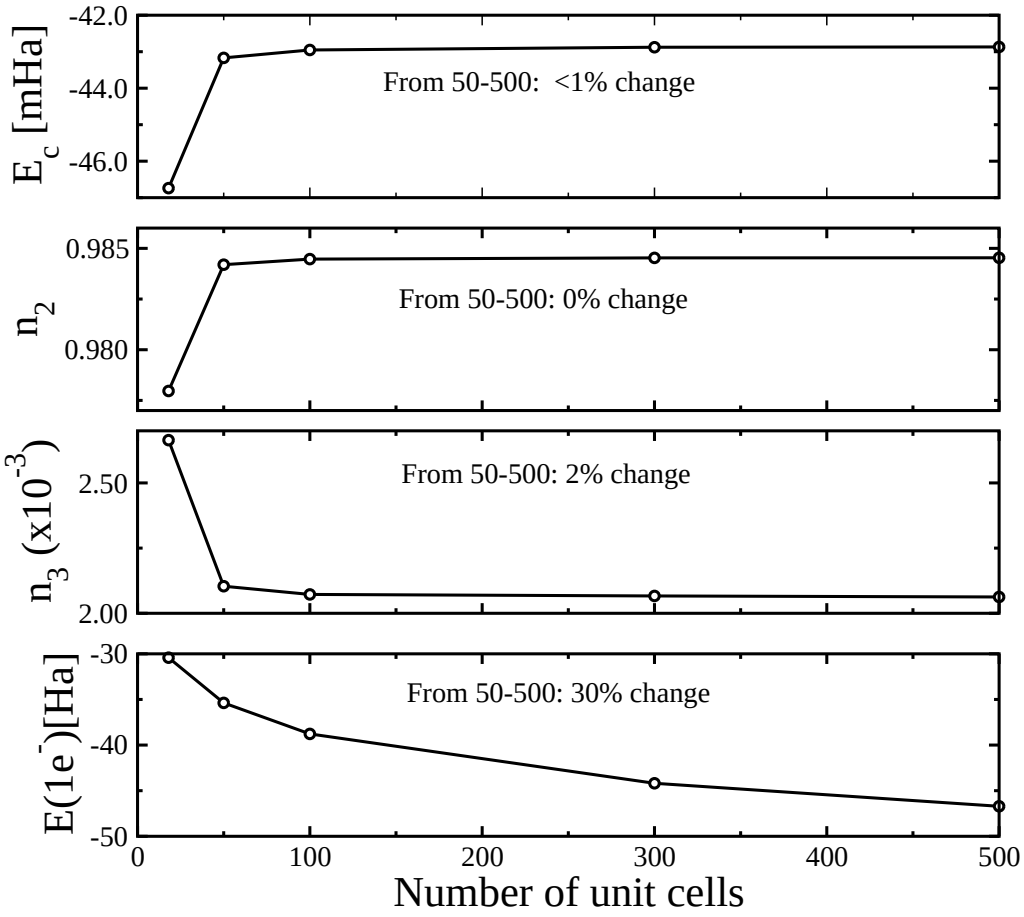

Figure 4.5: Correlation Energy, occupation numbers and one-electron energy as functions of the number of unit cells (on each side of the central cell) involved in the lattice summation.

Method	Total Energy [Ha]
HF (WANNIER)	-8.03806
HF + Perturbation[1]	-8.06874
HF (CRYSTAL)	-8.03803
LDA (VBH)[2]	-8.03840
LDA (VBH/VWN)[3]	-7.96821
GGA (PBE)[4]	-8.09456
GGA (PW91)[5]	-8.11031
B3LYP[6]	-8.12341
RDMFT(present)	-8.08213

Table 4.2: Total energy for the infinite LiH chain using various electronic structure methods.
[1]From Ref. [55] using Wannier code and the same basis set as the present work
[2]LDA from [56]
[3]exchange from [56] and correlation from [57]
[4]GGA from [3]
[5]GGA from [2]
[6]hybrid functional from [58]

all other results correspond to Bloch-state calculations using the CRYSTAL code [60] with the same Gaussian-type basis set as in the Wannier calculation. Our result is in excellent agreement with the GGA calculation.

4.4 Results for the Fundamental Gap

In Section 4.3.1 we have seen that the total energies of open- as well as closed-shell systems can be computed with high accuracy. We also discussed how to treat periodic systems by using Wannier states for the natural orbitals in Section 4.3.2. In this section we come back to the computation of the fundamental gap. The derivation in section 4.1 leading to Eq. (4.27) assumed that the exact exchange-correlation energy functional was available. Here, we investigate how approximate functionals perform in the calculation of the fundamental gap.

First, we consider the closed-shell molecule LiH using again the Goedecker/Umrigar functional. Fig. 4.6 shows the result of the numerical calculation of the chemical potential for different fractional particle numbers. There is a step near $M = 4$ which is sharp at the lower edge but relatively smooth at the upper edge. The discontinuity of $\mu(M)$ is located at a value slightly higher than $M = 4$ precisely at the point where the largest fractional occupation number becomes one and gets pinned. These features, the smoothness as well as the step at $M \neq 4$, are due to the approximate nature of the exchange-correlation energy. The exact functional yields

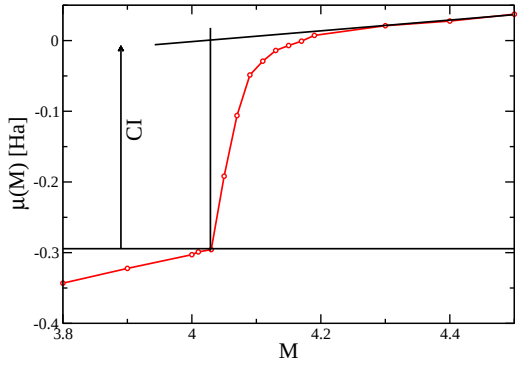

Figure 4.6: The chemical potential μ (in Hartree) as a function of particle number M for the LiH molecule calculated from the Goedecker/Umrigar functional.

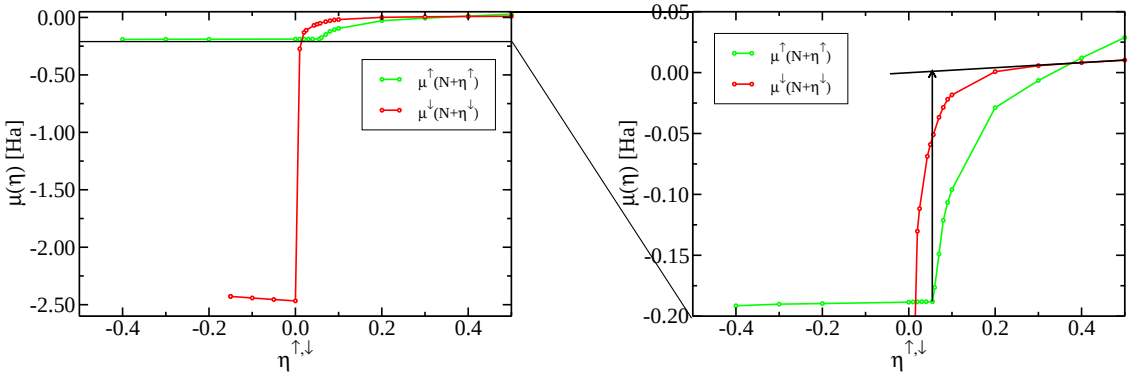

Figure 4.7: The two chemical potentials $\mu^{\uparrow}$ and $\mu^{\downarrow}$ (in Hartree) as a function of η for adding spin-up and spin-down electrons, respectively. The neutral system has a spin of $+1/2$. The right figure shows an enlargement of the left.

a step function with the discontinuity exactly at $M = 4$. In order to extract the gap from the graph in Fig. 4.6 we used the intersection of the extrapolated behaviour for $M > 4$ and a vertical line at the position of the jump. If the curve was a step function this procedure would yield the exact discontinuity.

For open-shell systems the situation is again more difficult. Fixing $N_{\uparrow}$ and $N_{\downarrow}$ separately, one has to distinguish between adding/subtracting spin-up or spin-down electrons. (For Li and Na, for example, the fundamental gap is given as the discontinuity between removing majority-spin electrons and adding minority-spin electrons.) Fig. 4.7 shows the chemical potentials $\mu^{\uparrow}(\eta^{\uparrow})$ and $\mu^{\downarrow}(\eta^{\downarrow})$ for adding η spin-up or spin-down electrons, respectively, to a neutral Li atom with spin $+1/2$. The graphs of $\mu^{\uparrow}(\eta^{\downarrow})$ and $\mu^{\downarrow}(\eta^{\uparrow})$ are omitted since they do not show any discontinuity. Since the neutral system contains two spin-up and one spin-down electron the gap is given by the discontinuity between $\mu^{\uparrow}$ for negative η and $\mu^{\downarrow}$ for positive η which is shown

System	RDMFT	Other theoretical	Experiment
Li	0.177	0.175[1]	0.175[2]
Na	0.175	0.169[3]	0.169[2]
LiH	0.296	0.286[4]	0.271[5]

Table 4.3: The fundamental gap for several atoms and small molecules calculated from the Goedecker/Umrigar functional.
[1] QCI from Ref. [49]
[2] from Ref. [61]
[3] Ionization potential from [49], electron affinity from [62]
[4] CISD using the same basis set as in RDMFT
[5] Ionization potential from [63], electron affinity from [64]

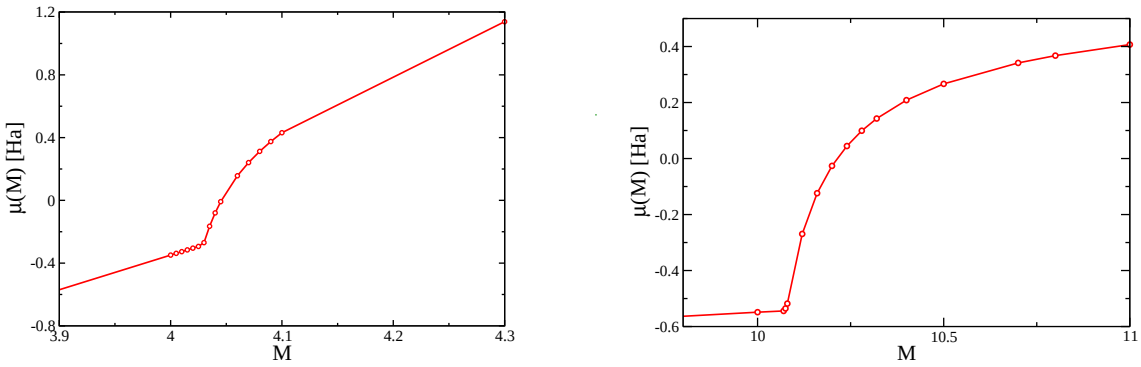

Figure 4.8: The chemical potential as a function of particle number for the one-dimensional LiH chain (left) and the three-dimensional Ne solid (right).

by the arrow in the right graph of Fig. 4.7. Calculations for Na yield results very similar to Fig. 4.7.

Table 4.3 compiles the results for all three systems, LiH, Li, and Na. It shows a remarkable agreement with both QCI results and experimental values for both open- as well as closed-shell systems.

As a first step towards calculating the band gap in realistic solids we consider a one-dimensional LiH chain. Employing again the GU approximation and using Wannier states as natural orbitals we obtain the chemical potential as a function of the particle number as shown in Fig. 4.8. Again, it shows a discontinuity close to $M = 4$. However, it is not as pronounced as for the molecule. The corresponding fundamental gap is given in Table 4.4. It is significantly larger than the LDA and GGA results obtained with the same basis set. Since both LDA and GGA are known to systematically underestimate the gap these results are encouraging. However, as the LiH chain does not exist in nature there are no experimental results for comparison.

The extension to three dimensional systems turns out to be extremely demanding

System	RDMFT	Other theoretical	Experiment
LiH chain	0.64	0.500(LDA), 0.509(GGA)	
Ne solid	0.76	0.439(LDA), 0.546(GGA)	0.797[1]

Table 4.4: The fundamental gap (in Hartree) for the one-dimensional LiH chain and three-dimensional solid Neon calculated from the Goedecker/Umrigar functional. The LDA and GGA calculations are performed using the same basis set as in the RDMFT calculation. [1] from Ref. [65]

with respect to computer memory. The Wannier orbitals need to be orthogonalized not only to their nearest but also to their next-nearest neighbours. In an fcc lattice this amounts to an orthogonalization to 12 nearest and 6 next-nearest neighbour lattice-sites which is numerically not feasible at present. Not performing these orthogonalizations leads to an unphysical energy. Therefore, as a first step, we consider a variation of the occupation numbers only. We keep the initial HF orbitals and calculate the optimal set of occupation numbers. The resulting chemical potential as a function of particle number is shown in Fig. 4.8. The chemical potential shows the typical discontinuity and a comparison with experiment, see Table 4.4, yields good agreement. This is not too surprising since it has been observed in other systems before that varying the occupation numbers only already leads to accurate results. The additional variation of the orbitals (when possible) modifies the band gap only marginally.